Preprints of the 18th IFAC World Congress
Milano (Italy) August 28 - September 2, 2011

Reconstruction of Plant Output from Quantized Measurement—A Moving Horizon Polynomial Fitting Approach

Hongzhong Zhu * **Toshiharu Sugie** *

* *Graduate School of Informatics, Kyoto University, Gokasho, Uji, Kyoto 611-0011, Japan (Tel: +81-774-383956; e-mail: zhu@robot.kuass.kyoto-u.ac.jp; sugie@i.kyoto-u.ac.jp).*

Abstract: This paper presents a new approach to reconstruct the plant output of linear time-invariant systems in the case where the available output measurement is quantized. By fitting the quantized measurement data with polynomials in a moving horizon manner, a smooth approximation of plant output is obtained via solving a convex optimization problem. Applying the signal to an observer, the plant output is reconstructed by taking account of the plant dynamics. It is guaranteed that the error between the true and the reconstructed output is bounded. Experimental validation is given by using a DC motor positioning system. It turns out that the proposed approach achieves small reconstruction error and accurate tracking control. In addition, the approach yields a smooth reconstruction signal so that the plant input is well behaved (or smooth) even if PID controller is employed for the plant subject to quantized output measurement.

Keywords: quantization error, output reconstruction, polynomial fitting, convex optimization

1. INTRODUCTION

Quantization in I/O signals is an inherent feature in many control systems including digital systems, networked ones, low resolution sensor/actuator systems, and so on. In some cases, the quantization error is substantially small compared to system noise or the desired position accuracy. However, this is not always the case. For instance, in most motion servo control systems, the optical encoders provide quantized measurement output and the quantization error may not be negligible. In this case, when the quantized measurement is used as the control signal directly, the quantization error will degrade the control accuracy or cause self-excited oscillations (Franklin et al. (1998)).

There is much literature focuses on understanding and suppression of quantization effects, see, e.g., Widrow et al. (1996), Zhang and Fu (2008). A simple classical approach to analyze and suppress the effects caused by quantization is to treat the quantization error as a bounded uncertainty and design a controller by applying robustness analysis tools (Fu (2005)). However, these methods commonly consider the worst-case conditions and it is difficult to find a nonconservative controller. Several researchers also propose some methods to estimate the system state based on the assumption that the quantization error is Gaussian noise. For instance, Van et al. (2004) present an adaptive Kalman filter to suppress the sensor quantization effects and demonstrate its effectiveness by the simulations. However, quantization behaves as highly colored noise and these methods are not always effective. Several numerical methods are also proposed to estimate the quantization error. Hirata and Kidokoro (2009) propose a quantization error estimator based on the least square method. However, the method is based on the assumption that the input disturbance is constant, which may be too restrictive in some cases. Besides, several approaches based on observer theory have been extensively studied, see Zhang and Fu (2008), Sur and Paden (1998), in which extra useful information is extracted from the quantized model and used to make a better estimation. Zhang and Fu (2008) propose a reset state estimator based on the information that the actual output is known exactly at the mid-point of the two consecutive quantizer levels; and Sur and Paden (1998) also present a projection algorithm to estimate the plant state based on the similar information. However, these methods commonly do not take account of the input disturbance and noise, which may not practical in real situation.

Due to the intrinsic feature of quantization, the error between the plant output and its quantized measurement is always bounded by the quantization level. Moreover, it is possible to get more precise information on the current true output from a series of past quantized measurement by taking account of the plant dynamics. This observation motivates us to consider a reconstruction of the plant output more precisely from the quantized measurement. In addition, it would be useful to obtain the smooth output signal, because it will yield the smooth plant input in the feedback systems even if the controller contains differential operation (such as PID). Therefore, a moving horizon curve fitting method is employed in this paper to take account of the smooth output reconstruction.

This paper is organized as follows. Section 2 introduces the system model and describes the problem settings. In section 3, the moving horizon polynomial fitting approach is presented, and the output reconstruction error is analyzed. Section 4 demonstrates the effectiveness of the proposed approach by using a DC motor positioning system. Finally, the conclusions are summarized in Section 5.

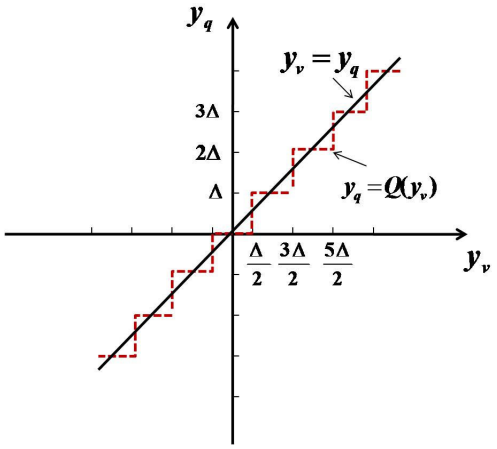

Fig. 1. Quantization characteristic; Δ: quantization level.

2. SYSTEM DESCRIPTION

Consider the linear time-invariant plant given by

$$\dot{x}(t) = Ax(t) + Bu(t) + w(t),\ x(0) = 0, \tag{1}$$

$$y(t) = Cx(t), \tag{2}$$

$$y_v(t) = y(t) + v(t), \tag{3}$$

$$y_q(t) = Q(y_v(t)), \tag{4}$$

where $A \in \mathbb{R}^{n\times n}, B \in \mathbb{R}^{n\times 1}$ and $C \in \mathbb{R}^{1\times n}$ are constant system matrices, and (C, A) is an observable pair. $x(t)$, $y(t)$, $y_v(t)$ and $y_q(t)$ are the state vector, the actual output, the corrupted output and the quantized measurement, respectively. $v(t) \in \mathbb{R}$ and $w(t) \in \mathbb{R}^n$ are the measurement noise and the input disturbance, respectively, which are assumed to be zero-mean and bounded by $\|w\|_\infty \le \gamma$, $\|v\|_\infty \le \delta$ for known γ and δ. The function $Q(\cdot)$ represents the uniform quantizer defined by

$$Q(y_v) = i \cdot \Delta,\ \ y_v \in ((i-0.5)\Delta, (i+0.5)\Delta], \tag{5}$$

where $i \in Z$, $\Delta > 0$ denotes the quantization level. We also assume that the quantization range is infinite. The relationship between y_v and y_q is shown in Fig. 1. In practical motion control systems, the quantizer (5) can be adopted to model the position sensor with quantization such as an incremental encoder, where Δ is also referred to as positioning resolution.

Due to the measurement noise $v(t)$, the difference between plant output $y(t)$ and the measured quantized output $y_q(t)$, which is denoted by $\xi(t) := y(t) - y_q(t)$, is bounded by

$$|\xi(t)| \le \frac{\Delta}{2} + \delta. \tag{6}$$

When the quantization level is large compared to the required specifications, the control performance could be degraded badly if the quantized measurement is directly used as the feedback signal. In addition, the plant input may exhibit wild behavior when the controller is high gain or has a derivative term. Therefore, a smooth, precise estimate of $y(t)$ would be preferred in practice. One of the most common ways to cope with the quantized measurement is to employ an observer and use its output instead of y_q itself, which is given by

$$\dot{\hat{x}}(t) = A\hat{x}(t) + Bu(t) + L(y_q(t) - \hat{y}(t)), \tag{7}$$

$$\hat{y}(t) = C\hat{x}(t), \tag{8}$$

where $\hat{x}$ and $\hat{y}$ are the estimated state and output, respectively, and $L \in \mathbb{R}^{n\times 1}$ is the observer gain. However, it is often the case that it does not work satisfactorily especially when the quantization level Δ is large. This motivates us to develop a new way to reconstruct $y(t)$ more precisely, which is outlined as follows:

First, we produce the smooth output estimate $\bar{y}$ by taking account of the following three points:

(a) It is possible to get more precise information on $y(t)$ from the past quantized measurement series $y_q(\tau)$ ($\tau \in [t-h\ \ t]$), where h is the given horizon;
(b) The quantization error is bounded by (6);
(c) The true output $y(t)$ should be smooth and band limited due to the plant dynamics.

Then, we use $\bar{y}$ instead of $y_q(t)$ in (7).

In the next section, we will present a moving horizon polynomial fitting approach, based on observer technique and convex optimization, to obtain a smooth reconstruction of the plant output by taking account of (a), (b) and (c).

3. MOVING HORIZON POLYNOMIAL FITTING APPROACH

In this section, firstly, a moving horizon polynomial fitting approach is presented to reconstruct the plant output. Then, we analyze the reconstruction error and show that the error is guaranteed to be bounded.

3.1 Polynomial fitting method

At first, we consider to fit the quantized measurement $y_q(t)$ in an interval, denoted by $[t_k - h\ \ t_k]$ (t_k is the current time and h is a fixed horizon), by using the polynomial

$$g_k(t) = \alpha_1 + \alpha_2 t + \cdots + \alpha_m t^{m-1},\ t \in [t_k - h\ \ t_k], \tag{9}$$

where $\alpha_1\ \alpha_2\ \cdots\ \alpha_m$ is the coefficients to be determined, and m is the dimension of the polynomial. The polynomial can also be regarded as an approximate signal of plant output in $[t_k - h\ \ t_k]$. We handle this fitting problem by the following two steps:

- Sample p data from the quantized measurement $y_q(t)$ in $[t_k - h\ \ t_k]$ with a fixed sampling period T_s (so that the fixed horizon can be set as $h := (p-1)T_s$);
- Form the vector of errors as follows:

$$v = \begin{bmatrix} g_k(t_k - (p-1)T_s) - y_q(t_k - (p-1)T_s) \\ \vdots \\ g_k(t_k - iT_s) - y_q(t_k - iT_s) \\ \vdots \\ g_k(t_k) - y_q(t_k) \end{bmatrix},$$

where $i = p-1, p-2, \cdots, 0$, and minimize it via ℓ_2-norm

$$\underset{\alpha}{\text{minimize}}: \quad \|v\|_2 \tag{10}$$

with variables $\alpha = [\alpha_1\ \alpha_2\ \cdots\ \alpha_m]^T$.

The problem (10) is to minimize the error between the polynomial and sampled data at every sampling time in $[t_k - h\ \ t_k]$ via ℓ_2-norm. It can be expressed as

$$\underset{\alpha}{\text{minimize}}: \quad \|v\|_2 = \|T(t_k)\alpha - b\|_2. \tag{11}$$

with variable α, where $T(t_k)_{ij} = (t_k - (p-i)T_s)^{j-1}$, $b_i = y_q(t_k - (p-i)T_s)$, $i = 1, 2, \cdots, p$, $j = 1, \cdots, m$. α can be calculated if

this problem is solved. In general, high-degree high-dimension polynomial function can lead to erroneous fitting, such as that it can arouse overshoot and swing through wild oscillations (G. Strang (1986)). Therefore, we consider to set a proper high dimension for polynomial (9) and use some heuristics to reduce the dimension automatically, namely, take some function on α to get a sparse solution. Since ℓ_1-norm puts relatively larger emphasis on small residuals and can get a sparse solution (Boyd and Vandenberghe (2004)), we adopt ℓ_1-norm here and the fitting problem is reformed as

$$\underset{\alpha}{\text{minimize}}: \quad \|T(t_k)\alpha - b\|_2 + \eta\|\alpha\|_1, \tag{12}$$

with variable $\alpha \in \mathbb{R}^m$, where η is the weighting factor.

3.2 Moving horizon curve fitting

At time t_k, $y_q(t_k)$ is sampled from the quantized output, and the polynomial (9) is determined by solving the problem (12). As we described above, the polynomial can be regarded as an approximate signal of the plant output in the interval $[t_k - h \;\; t_k]$. Therefore, the approximation value of the plant output at t_k, denoted by $\bar{y}(t_k)$, is calculated by

$$\bar{y}(t_k) = g_k(t_k). \tag{13}$$

On the real-time calculation, when the current time t_k is updated, say, from t_k to t_{k+1} according with a sampling period T_s, a new quantized measurement $y_q(t_{k+1})$ is sampled as well as the matrix $T(t_k)$ and vector b in problem (12) are renewed, a new polynomial $g_{k+1}(t)$ will be calculated again (in the new internal $[t_{k+1} - h \;\; t_{k+1}]$). The immediate approximation value of the plant output at t_{k+1} is determined by $\bar{y}(t_{k+1}) = g_{k+1}(t_{k+1})$. In the case of $k \leq p$, we set $y_q(k-i) = 0$ for $i = k, k+1, \cdots, p$ as the initialization. By doing this, a discrete signal $\bar{y}(t_i)$ can be obtained by successively repeating the fitting procedures and solving (13). The sampling period T_s is assumed to be small, the signal $\bar{y}(t_i)$ $(i = 1, 2, \cdots)$ therefore can be regarded as a continuous signal, which is denoted by $\bar{y}(t)$ for the sake of convenience.

In order to improve the approximate accuracy between $\bar{y}(t)$ and plant output $y(t)$, several constraint conditions of the problem (12) is considered here. As described in Section 2, the difference between the plant output and the quantized output is always bounded according to (6). Therefore, the constraint condition

$$|g_k(t_k) - y_q(t_k)| < \frac{\Delta}{2} + \delta \tag{14}$$

can be added to the problem (12). In addition, in order to obtain a smooth approximate signal $\bar{y}(t)$, the following two conditions

$$g_k(t_{k-1}) = \bar{y}(t_{k-1}), \tag{15}$$

$$\dot{g}_k(t_{k-1}) = \dot{\bar{y}}(t_{k-1}). \tag{16}$$

where $\dot{g}_k(t_{k-1})$ is the slope of the polynomial (9) at time index t_{k-1}, is also considered. These conditions imply that $\bar{y}(t_{k-1})$ and $\bar{y}(t_k)$ are smoothly connected via polynomial $g_k(t)$. However, the approximate accuracy may be degraded if the new approximate value $\bar{y}(t_k)$ is determined based on last approximate value $\bar{y}(t_{k-1})$. Therefore, we employ the observer

$$\dot{\hat{x}}(t) = A\hat{x}(t) + Bu(t) + L(\bar{y}(t) - \hat{y}(t)) \tag{17}$$

$$\hat{y}(t) = C\hat{x} \tag{18}$$

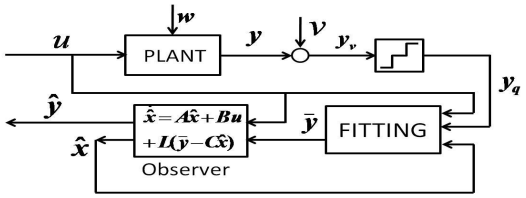

Fig. 2. Block diagram of output reconstruction scheme. $\hat{y}$ is regarded as the reconstruction signal of actual output y.

where $L \in \mathbb{R}^{n\times 1}$ is the observer gain which is designed to stabilize $A - LC$, to estimate the plant state, and the following conditions

$$\dot{g}_k(t_{k-1}) = CA\hat{x}(t_{k-1}) + CBu(t_{k-1}) \tag{19}$$

$$g_k(t_{k-1}) = C\hat{x}(t_{k-1}) \tag{20}$$

are used instead of (15) (16) to make sure that $\bar{y}(t_k)$ and $\bar{y}(t_{k-1})$ are smoothly connected.

From above, we can organize the polynomial fitting problem as

$$\underset{\alpha}{\text{minimize}}: \quad \|T(t_k)\alpha - b\|_2 + \eta\|\alpha\|_1 \tag{21}$$

subject to:

(14), (19), (20)

with variable $\alpha \in \mathbb{R}^m$. It is obvious that the objective function and the inequality constraint function (left part of (14)) are convex, and the equality constraint functions (left parts of (19), (20)) are affine. Therefore, the minimization problem is a convex optimization problem and can be solved efficiently. Note that the three constraint conditions are independent with each other, so that the problem is feasible if the polynomial (9) has the dimension not less than 3 ($m \geq 3$). When the problem (21) is solved, the approximate signal $\bar{y}(t)$, which is used by the observer (17), can be calculated by (13). We regard $\hat{y}(t)$ obtained by the observer as the reconstruction signal of $y(t)$. The block diagram of the reconstruction scheme is shown in Fig. 2.

3.3 Reconstruction Error Analysis

Finally, we will analyze how "big" the reconstruction error is when the proposed approach is applied. For convenience, the reconstruction error is defined by

$$\mathrm{e}_r(t) := y(t) - \hat{y}(t).$$

In addition, we analyze the error on continuous-time series by assuming that the sampling period is small.

From the inequalities (14) and (6), we know that the difference between the approximation signal $\bar{y}(t)$ and the plant output $y(t)$, denoted by

$$\zeta(t) := \bar{y}(t) - y(t), \tag{22}$$

is bounded by

$$|\zeta(t)| < \Delta + 2\delta. \tag{23}$$

Describe the state estimate error as

$$e_x(t) := x(t) - \hat{x}(t), \tag{24}$$

and thus, subtracting the equation (17) from the plant (1) derives the state error system with the dynamic equation

$$\begin{cases} \dot{e}_x(t) = \tilde{A}e_x(t) + w(t) - L\zeta(t), \\ e_r(t) = Ce_x(t) \end{cases} \tag{25}$$

where $\tilde{A} = A - LC$, which is stable. This error system can be divided into following two subsystems

$$G_w : \begin{cases} \dot{e}_{x1}(t) = \tilde{A}e_{x1}(t) + w(t), \\ e_{r1}(t) = Ce_{x1}(t) \end{cases} \tag{26}$$

$$G_\zeta : \begin{cases} \dot{e}_{x2}(t) = \tilde{A}e_{x2}(t) - L\zeta(t), \\ e_{r2}(t) = Ce_{x2}(t) \end{cases} \tag{27}$$

with $e_x(t) = e_{x1}(t) + e_{x2}(t)$ and $e_r(t) = e_{r1}(t) + e_{r2}(t)$.

Then we have

$$e_{r1}(t) = \int_0^t g_w(t-\tau)w(\tau)d\tau, \tag{28}$$

$$e_{r2}(t) = \int_0^t g_\zeta(t-\tau)\zeta(\tau)d\tau \tag{29}$$

where $g_w(t)$ and $g_\zeta(t)$ are the convolution kernel. Since $w(t)$ is assumed as $\|w(t)\|_\infty \le \gamma$, thus the error $e_{r1}(t)$ is bounded by

$$\begin{aligned} \|e_{r1}(t)\| &= \| \int_0^t g_w(t-\tau)w(\tau)d\tau\| \le \int_0^t \|g_w(t-\tau)w(\tau)\|d\tau \\ &\le \int_0^t \|g_w(\tau)\|d\tau \, \|w\|_\infty \le \int_0^t \|g_w(\tau)\|d\tau \, \gamma. \end{aligned}$$

Therefore, $\|e_{r1}\|_\infty \le \int_0^\infty \|g_w(\tau)\|d\tau \, \gamma$. Using the theorem 4.5 of K. Zhou's book (1995), we can have $\int_0^\infty \|g_w(\tau)\|d\tau \le 2\sum_{i=1}^n \sigma_{w_i}$, where $\sigma_{w_1} \ge \sigma_{w_2} \ge \cdots \ge \sigma_{w_n} \ge 0$ are the Hankel singular values of subsystem G_w. And thus the inequality

$$\|e_{r1}\|_\infty \le 2\gamma \sum_{i=1}^n \sigma_{w_i},$$

is obtained. Similarly, we can have

$$\|e_{r2}\|_\infty \le 2(\Delta + 2\delta) \sum_{i=1}^n \sigma_{\zeta_i},$$

where $\sigma_{\zeta_1} \ge \sigma_{\zeta_2} \ge \cdots \ge \sigma_{\zeta_n} \ge 0$ are the Hankel singular values of subsystem G_ζ. Therefore, the following inequalities

$$\begin{aligned} \|e_r(t)\|_\infty &\le \|e_{r1}\|_\infty + \|e_{r2}\|_\infty \\ &\le 2\gamma \sum_{i=1}^n \sigma_{w_i} + 2(\Delta + 2\delta) \sum_{i=1}^n \sigma_{\zeta_i} \end{aligned}$$

are obtained, which means that the reconstruction error is guaranteed to be bounded.

4. EXPERIMENTS

This section demonstrates the application of the moving horizon polynomial fitting approach to a DC motor control system with an optical encoder of 22 μm resolution. Fig. 3 shows the experimental setup. Experimental results are shown to verify the effectiveness of the proposed approach (MHPFA) over the standard state estimator (SSE) without fitting process.

The model of DC motor is obtained by an identification experiment, which is described by

$$\begin{bmatrix} \dot{x} \\ \ddot{x} \end{bmatrix} = \begin{bmatrix} 0 & 1 \\ 0 & -69.623 \end{bmatrix} \begin{bmatrix} x \\ \dot{x} \end{bmatrix} + \begin{bmatrix} 0 \\ 9.2543 \end{bmatrix} u,$$

$$y = \begin{bmatrix} 1 & 0 \end{bmatrix} \begin{bmatrix} x \\ \dot{x} \end{bmatrix}.$$

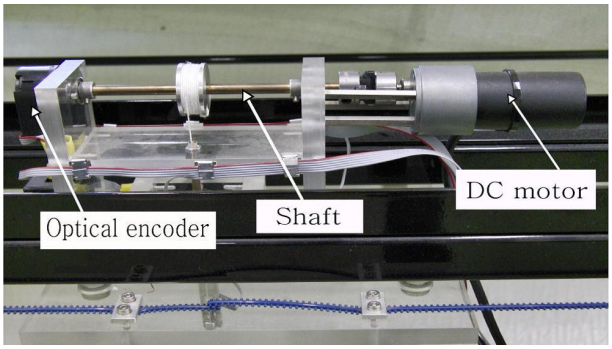

Fig. 3. Experimental setup.

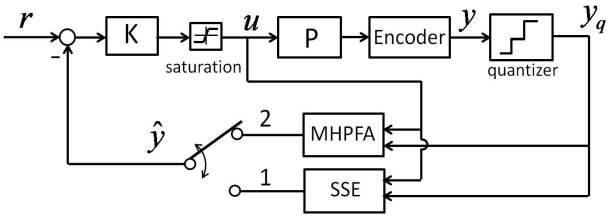

Fig. 4. Block diagram of DC motor control system: y is measured by the optical encoder, a software quantizer is introduced to simulate the low-resolution encoder, the motor input is limited in $[-1\ 1]V$. Case 1: the standard state estimator is used; Case 2: the proposed method is used.

where x is the position and $\dot{x}$ is the velocity. The controller is given by

$$K(s) = k_p + k_d \frac{s}{0.004s + 1} + k_i \frac{1}{s} \tag{30}$$

where $k_p = 800$, $k_d = 5$, $k_i = 50$. Note that the controller owns a high gain and a derivative term. The block diagram of the LTI control system is shown in Fig. 4. The input of the motor is limited in $[-1\ \ 1]$V. The position signal measured by the optical encoder is regarded as the actual position y. To verify the effectiveness the proposed approach, a software quantizer is introduced to simulate a low resolution encoder. The quantized output y_q together with the control input u are then used as the inputs of MHPFA and SSE. For comparison, the reconstruction output $\hat{y}$ from SSE (Case 1) and MHPFA (Case 2) are respectively used as the feedback signals. The sampling period of the control system is set as $T_s = 1\ ms$.

In the setup, the quantization level is set as $\Delta = 3\ cm$. The noise $v(t)$ is set as $v \le \delta$, where $\delta = 0.05\ cm$. The observer gain L is calculated by properly placing the poles at -10, -12 (the same with the SSE method). In addition, the initial value of matrix T and the vector b in (21) is set as $T(0) = 0$ and $b = 0$, the fitting data number p, the dimension of the polynomial m, and the weighting factor η is properly set as $p = 30$, $m = 5$, and $\eta = 1 \times 10^{-3}$, respectively.

For the sake of comparison, the reconstruction error e_r and position tracking error E_c are respectively defined as

$$e_r = y - \hat{y}, \tag{31}$$

$$E_c = r - y. \tag{32}$$

The controller is modeled by a Simulink block, and the C code of the minimization problem (21) is generated by using CVXGEN (J. Mattingley et al. (2010)). In the case of $p = 30$

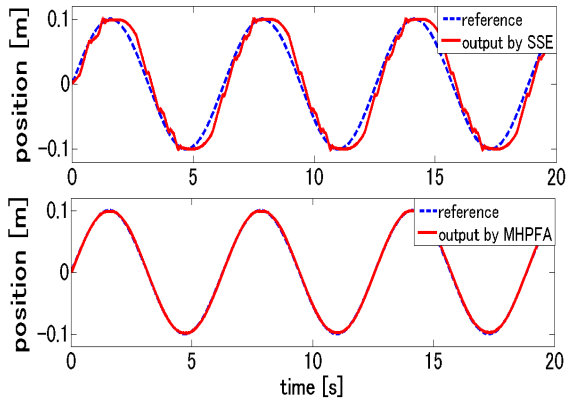

Fig. 5. Comparison between reference r and plant output y. Solid lines: reference input, Dashed lines: the plant output obtained by SSE and MHPFA, respectively.

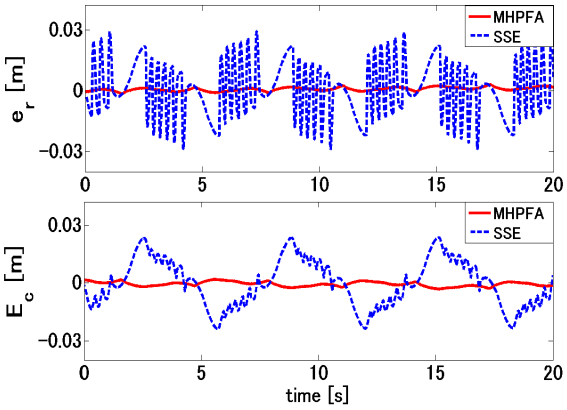

Fig. 6. The comparison of reconstruction error and position tracking error caused by MHPFA approach and SSE method. Solid lines: the error obtained by MHPFA, Dashed lines: the error obtained by SSE.

and $m = 5$, the computational time of solving the problem (21) can be as small as 60 μs (Intel Core 2 Duo CPU L7100 @ 1.20 GHz with 2 GB of memory), which means that it is sufficient to solve the minimization problem during the sampling period.

The reference input r is set as the sinusoidal signal $r = 10\sin t\ cm$ and the experiment is performed. The experimental results are shown in Fig. 5 $\sim$ 7. Fig. 5 shows the comparison between reference input $r(t)$ and plant output $y(t)$ achieved by MHPFA and SSE. The reconstruction error and position tracking error caused by MHPFA and SSE are shown in Fig. 6. It is obvious that MHPFA can achieve a better tracking accuracy and obtain a good plant output reconstruction. In addition, by using the proposed approach, a smooth plant input is achieved even if the controller owns a high gain and a derivative term. Fig. 7 shows the comparison of plant input obtained by the MHPFA approach and SSE method. We know that the motor behaves more softly when the proposed approach is used. The maximum amplitudes and RMS of the reconstruction error and the position tracking error E_c in one period ($t = 0\ [s]$ to $t = 2\pi\ [s]$) are shown in Table 1 and Table 2. It is observed that the maximum of reconstruction error and tracking error versus quantization level are below 10%. Therefore, the quantization effects are shown to be suppressed by the proposed approach.

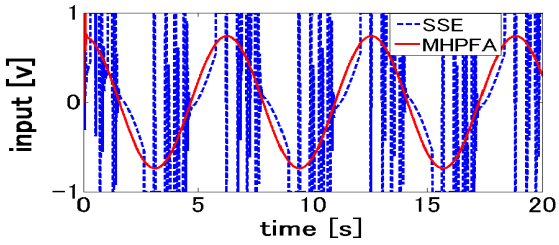

Fig. 7. The comparison of input $u(t)$ of MHPFA approach and SSE method.

Table 1. Maximum Amplitude and RMS of reconstruction error e_r

	SSE	MHPFA
max err $[cm]$	2.93	0.16
RMS $[cm]$	1.30	0.071
max err/Δ	97.7 %	5.3 %

Table 2. Maximum Amplitude and RMS of position tracking error E_c

	SSE	MHPFA
max err $[cm]$	2.39	0.21
RMS $[cm]$	1.24	0.11
max err/Δ	79.7 %	7.0 %

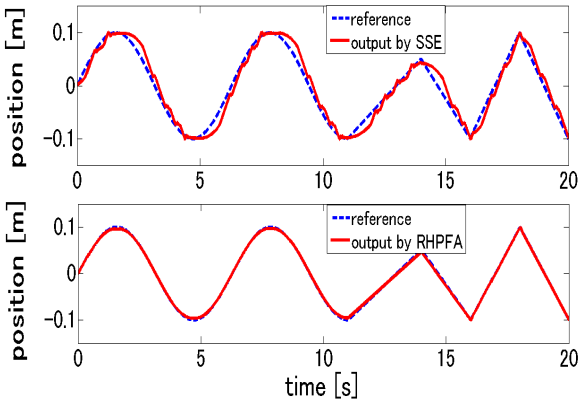

Fig. 8. The comparison of reference and plant output obtained by MHPFA and SSE in the case that reference input is switched to triangle wave at $t = 11\ [s]$. Solid lines: reference input, Dashed lines: the plant output obtained by SSE and MHPFA, respectively.

To verify the robustness of the proposed approach against the reference input, we switch the reference input from sinusoidal signal $r(t) = 10\sin(t)$ to triangle wave signal at $t = 11\ [s]$. The experiment results are shown in Fig. 8 $\sim$ 10. Fig. 8 shows the comparison between reference input $r(t)$ and plant output $y(t)$ achieved by MHPFA and SSE. The reconstruction error and position tracking error caused by MHPFA and SSE are shown in Fig. 9. Besides, the comparison of plant input obtained by the MHPFA approach and SSE method is shown in 10. It is observed that the reconstruction performance is not deteriorated when the reference signal is switched. Therefore, the effectiveness of the proposed approach is verified.

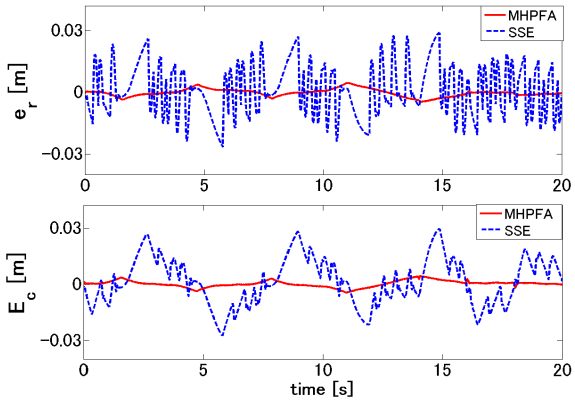

Fig. 9. The comparison of reconstruction error and position tracking error obtained by MHPFA and SSE in the case that reference input is switched to triangle wave at t = 11 [s]. Solid lines: the error obtained by MHPFA, Dashed lines: the error obtained by SSE.

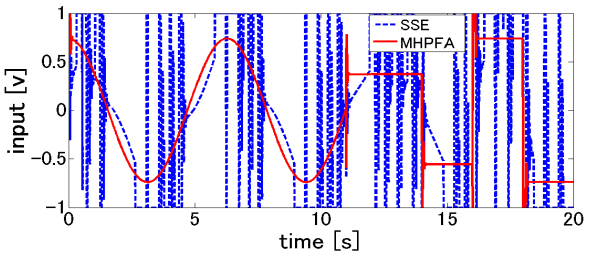

Fig. 10. The comparison of input $u(t)$ between MHPFA and SSA in the case that the reference is switched to triangle wave at t = 11 [s].

5. CONCLUSION

We have proposed a new method to reconstruct the plant output of SISO linear time-invariant systems from the quantized measurement. It exploits the moving horizon polynomial fitting approach with some additional constraints, which takes account of the quantization level and smoothness of the estimated output. The approach is based on a standard observer and convex optimization technique, and therefore it is computationally tractable. The experimental results are given to demonstrate the effectiveness of the proposed approach. Note that the approach does not depend on any specific control structures, so that it could be combined with any type of control methods.

ACKNOWLEDGEMENTS

The authors would like to thank Prof. Stephen Boyd and Jocob Mattingley for providing C code generator for the convex optimization problem.

REFERENCES

B. Widrow, I. Kollar, and M. Liu. Statistical Theory of Quantization. *IEEE Trans. Automat. Contr.*, 45: 353–356, Apr. 1996.

D. L. Van, M. Tordon, J. Katupitiya. Covariance Profiling for an Adaptive Kalman filter to Suppress Sensor Quantization Effects. *Proc. IEEE Conf. Decision and Control*, 2680–2685, 2004.

F. Franklin, J. D. Powell, M. Workman. *Digital Control of Dynamic Systems*, 3rd edition, Addison-Wesley, 1998.

G. Strang. *Introduction to Applied Mathematics*, Wellesley, Cambridge Press, 1986.

J. Mattingley, Y. Wang, S. Boyd. Code Generation for moving horizon Control. *Proceedings IEEE Multi-Conference on Systems and Control*, pp. 985-992, Yokohama, Japan, Sep.,2010.

J. Sur, and B. E. Paden. State Observer for Linear Time-Invariant Systems With Quantized Output. *Journal of Dynamic Systems, Measurement, and Control*, Vol. 120: 423-426, Sep.1998

J. Zhang, M. Fu. A Reset State Estimator for Linear Systems to Suppress Sensor Quantization Effects. Proc. 17th IFAC World Congress, 2008.

K. Zhou with J.C. Doyle and K. Glover. *Robust and Optimal Control*, Prentice-Hall, 1995.

M. Fu, L. Xie. The Sector Bound Approach to Quantized Feedback Control. *IEEE Trans. Automat. Contr.*, Vol. 50, NO. 11, Nov. 2005.

M. Hirata, T. Kidokoro. Servo Performance Enhancement of Motion System via a Quantization Error Estimation Method–Introduction to Nanoscle Servo Control. *IEEE Trans. on Industrial Electronics*, Vol. 56, No. 10, Oct. 2009.

S. Boyd, L. Vandenberghe. *Convex Optimization*, Cambridge University Press, 2004.